International Journal of Nanomedicine

Dovepress
open access to scientific and medical research

Open Access Full Text Article

ORIGINAL RESEARCH

Counteracting the effect of leukemia exosomes by antiangiogenic gold nanoparticles

This article was published in the following Dove Press journal:
International Journal of Nanomedicine

Catarina Roma-Rodrigues
Alexandra R Fernandes
Pedro V Baptista

UCIBIO, Departamento de Ciências da Vida, Faculdade de Ciências e Tecnologia, Universidade NOVA de Lisboa, Campus de Caparica, Caparica 2829-516, Portugal

Purpose: Progression of chronic myeloid leukemia (CML) is frequently associated with increased angiogenesis at the bone marrow mediated by exosomes. The capability of gold nanoparticles (AuNPs) functionalized with antiangiogenic peptides to hinder the formation of new blood vessels has been demonstrated in a chorioallantoic membrane (CAM) model.

Methods: Exosomes of K562 CML cell line were isolated and their angiogenic effect assessed in a CAM model. AuNPs functionalized with antiangiogenic peptides were used to block the angiogenic effect of CML-derived exosomes, assessed by evaluation of expression levels of key modulators involved in angiogenic pathways - *VEGFA, VEGFR1* (also known as *FLT1*) and *IL8*.

Results: Exosomes isolated from K562 cells promoted the doubling of newly formed vessels associated with the increase of *VEGFR1* expression. This is a concentration and time-dependent effect. The AuNPs functionalized with antiangiogenic peptides were capable to block the angiogenic effect by modulating *VEGFR1* associated pathway.

Conclusion: Exosomes derived from blast cells are capable to trigger (neo)-angiogenesis, a key factor for the progression and spreading of cancer, in particular in CML. AuNPs functionalized with specific antiangiogenic peptides are capable to block the effect of the exosomes produced by malignant cells via modulation of the intrinsic VEGFR pathway. Together, these data highlight the potential of nanomedicine-based strategies against cancer proliferation.

Keywords: chronic myeloid leukemia, exosomes, chorioallantoic membrane, gold nanoparticles, angiogenesis

Introduction

Chronic myeloid leukemia (CML), characterized by the uncontrolled proliferation of myeloid cells, has an incidence of 1–2 cases per 100,000 adults and accounts for circa 15% of newly diagnosed leukemia cases in adults.[1] CML is caused by the fusion of the Abelson murine leukemia (*ABL1*) gene on chromosome 9 with the breakpoint cluster region (*BCR*) gene on chromosome 22, forming an aberrant chromosome designated by Philadelphia chromosome.[2] This translocation results in a *BCR-ABL1* fusion gene encoding a tyrosine kinase with permanent-elevated activity, resulting in enhanced cell proliferation.[2] CML patients initial treatment rely on tyrosine kinase inhibitors that block the aberrant fusion protein.[1] This aberrant proliferation, in turn, triggers a range of cell and molecular events in the bone marrow, which correlate with disease progression and prognosis.[3] In the bone marrow tumor microenvironment, autocrine and paracrine communication between malignant cells and bone marrow cells are crucial for modulation and evolution of the niche.[3,4] For example, it has been previously reported the direct correlation

Correspondence: Alexandra R Fernandes; Pedro V Baptista
UCIBIO, Departamento de Ciências da Vida, Faculdade de Ciências e Tecnologia, Universidade NOVA de Lisboa, Campus de Caparica, Caparica 2829-516, Portugal
Tel +351 21 294 8530
Fax +351 21 294 8530
Email ma.fernandes@fct.unl.pt; pmvb@fct.unl.pt

submit your manuscript | www.dovepress.com
DovePress
http://doi.org/10.2147/IJN.S215711

between blast transformation and the caliber and density of microvessels in the bone marrow.[3]

Exosomes are small vesicles with 30–100 nm diameter formed in the endosomal pathway, usually composed by a lipid bilayer containing membrane proteins capable to encapsulate nucleic acids, such as mRNA and miRNAs, proteins and several other molecules involved in cellular communication (eg, cytokines and growth factors).[5,6] After release to the extracellular milieu, exosomes are pivotal for the communication between adjacent cells and for endocrine communication upon entering circulation (blood and lymph).[7,8] It has also been demonstrated the capability of exosomes to trigger (neo)-angiogenesis, a crucial step for the progression and evolution of cancer.[9–11] Perhaps the most striking feature of exosomes is their ability to alter the phenotype of secondary cells once they internalize.[12]

Regarding exosomes secreted by CML cells, several reports have demonstrated their capability to induce the formation of new vessels, suggesting their role in neo-angiogenesis in the bone marrow of CML patients.[11,13–18] Despite the mechanisms involved in this event not being fully understood, several key molecules involved in angiogenesis have been identified within exosomes derived from CML, such as the pro-angiogenic miRNAs, miR-92, and miR126.[13,18] Moreover, K562 derived exosomes were found to induce angiotube formation in human umbilical endothelial cells (HUVEC) in a SRC-dependent way.[14] Also, exosomes secreted by LAMA84 CML cells induced the expression of interleukin-8 (IL-8) in HUVEC.[11] More recently, Conrado et al, found that exosomes collected from blood from CML patients contain amphiregulin, which activates epidermal growth factor receptor (EGFR) in stromal cells located in the bone marrow.[16] Stromal cells activated through EGFR secret IL-8, which then stimulates the proliferation of CML cells.[16]

Nanomedicine has been putting forward several innovative therapeutic tools to manage hematological malignancies.[4,19] Particularly, the versatility of nanoparticles makes them suitable for use in a large range of applications, from imaging and diagnosis to therapy.[4,19,20] It has been proposed that the enhanced permeability and retention effect at the tumor location, resulting in altered endothelial, potentiates nanomedicines accumulation at the site, with concomitant improvement to drug delivery and efficacy.[4,19,20]

We have previously shown that gold nanoparticles (AuNPs) designed to interact with neuropilin-1 receptor (NRP-1) were effective at modulating angiogenesis in vitro and in vivo without toxicity.[21–24] In fact, by using a chorioallantoic membrane (CAM) model, it was shown that an 86% decrease of newly formed arterioles was possible upon delivery of antiangiogenic AuNPs, whose effect could be further potentiated by the direct laser irradiation.[21,22] The exact role of membrane glycoprotein NRP-1 in angiogenesis is still not completely understood but it is accepted that NRP-1 enhances the binding of the vascular endothelial growth factor (VEGF) to VEGF receptors 1 and 2 (VEGFR-1 and VEGFR-2).[25]

Here, the potential of antiangiogenic AuNPs to circumvent the effect of CML-derived exosomes in triggering the development of new vessels was evaluated (Figure 1).

Materials and methods

Cell cultures and cell cultures maintenance

The CML cell line K562 (ATCC Cat# CCL-243, RRID: CVCL_0004, Manassas, VA, USA), with the *BCR-ABL1* e14a2 fusion transcript, and the human primary dermal normal fibroblasts, neonatal (ATCC Cat# PCS-201–010, Lot: 61728499) were cultured on Dulbecco's modified eagle medium (DMEM, ThermoFisher Scientific, Waltham, Massachusetts, USA) supplemented with 10% (v/v) heat-inactivated fetal bovine serum (FBS, ThermoFisher Scientific) and a mixture of 100 U/mL Penicillin and 100 µg/mL Streptomycin (ThermoFisher Scientific). Cultures were maintained at 37°C, 5% (v/v) CO_2, and 99% (v/v) relative humidity.

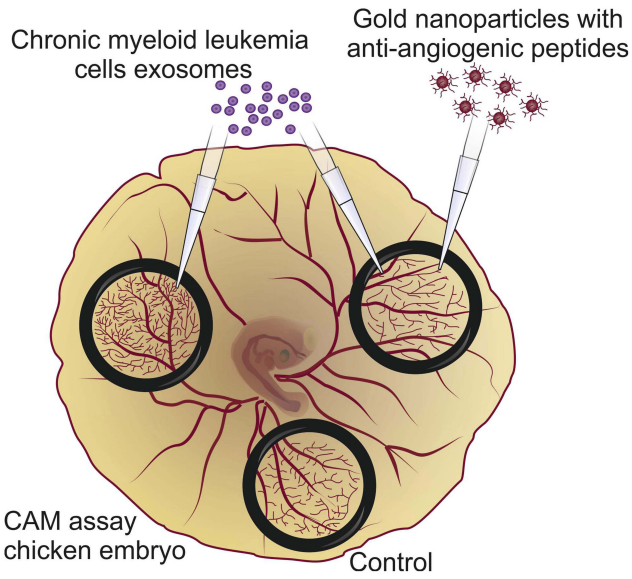

Figure 1 Antiangiogenic gold nanoparticles block the chronic myeloid leukemia (K562) derived exosomes induced angiogenesis.

Exosome isolation and characterization

Cell cultures for exosome isolation

When Fibroblast cultures reached 80% confluency, cells were detached using Tryple Express (ThermoFisher Scientific), centrifuged at 300×g for 5 mins, washed two times with phosphate buffer saline (PBS), and 1×10^5 cells were seeded in T-flasks with 25 cm^2 area containing 5 mL DMEM supplemented with 10% (v/v) heat-inactivated exosome depleted FBS (ThermoFisher Scientific). After 24 hrs incubation, to ensure that cells adhere to the flask surface, the medium was replaced by 5 mL identical fresh medium and cells were incubated for 72 hrs. The supernatant was then collected, centrifuged at 3000×g to remove cell debris and stored at −80°C until use.

When K562 cultures reached a density of 1×10^6 cells/mL, cells were pelleted by a centrifugation of 300×g, 5 mins and washed three times with PBS. Cells were then seeded in a density of 2×10^5 cells/mL in T-flasks with 25 cm^2 area containing 5 mL DMEM supplemented with 10% (v/v) heat-inactivated exosome depleted FBS. After 72 hrs incubation, the supernatant was collected, centrifuged at 3000×g to remove cells and cell debris and stored at −80°C until use.

Exosome isolation

For exosome isolation, supernatants were slowly thawed and filtered by a syringe filter with 0.2 µm diameter. The filtered solution was concentrated in a Centrifugal device with 3KD pore (PALL, New York, USA) and resultant suspension (concentrated solution) was mixed with Total exosome isolation reagent (from cell culture media, ThermoFisher Scientific) according to manufacturer's instructions. After 15 hrs incubation at 4°C, the mixture was centrifuged at 10,000×g, 1 hr, 4°C, the supernatant was completely removed, and pelleted exosomes were solubilized in PBS. Exosomes were stored at –80°C until needed.

The successful exosome isolation was confirmed by the presence of CD-81 in samples and by dynamic light scattering (DLS). The total protein concentration in the exosome solutions was measured using the Pierce 660 nm Protein Assay reagent (ThermoFisher Scientific).

Western-blot for CD-81 detection

For Western-blot analysis, 30 µg protein of concentrated solution of K562- and fibroblasts-derived exosomes suspensions was mixed with loading buffer (70 mM Tris-HCl, pH 6.8, 10% (v/v) Glycerol, 1% (w/v) sodium dodecyl sulfide (SDS), 1% (w/v) Dithiothreitol and 0.005% (w/v) bromophenol blue) and incubated for 2 hrs at room temperature. Afterward, proteins were separated in an SDS-polyacrylamide gel electrophoresis (SDS-PAGE) using a 10% (w/v) polyacrylamide gel with 37.5:1 ratio of acrylamide: bisacrylamide and then transferred to a 0.45 µm PVDF membrane (GE Healthcare, Chicago, Illinois, USA). Resultant membrane was stained with Ponceau S solution (Biotium, Fremont, California, USA) according to manufacturer´s instructions and incubated with 5% (w/v) non-fat dry milk in TBST (Tris-buffer saline with 0.1% (v/v) Tween-20) for 2 hrs at room temperature and for 2 hrs at 4°C. Blots were then incubated over-night at 4°C with CD-81 antibody (1D6, Novus biologicals Cat# NB100-65,805, RRID: AB_962702, Littleton, Colorado, USA) in a final concentration of 1.5 µg/mL in 5% (w/v) non-fat dry milk in TBST, washed three times with TBST and incubated for 1 hr with secondary antibody anti-mouse IgG, HRP-linked antibody (Cell Signaling Technology Cat#7076, RRID:AB_330924, Danvers, Massachusetts, USA). After washing three times with TBST, blots were treated with Westernbright ECL HRP substrate (Advansta, San Jose, California, USA) and visualized by exposing the blots in a Hyperfilm ECL (GE Healthcare).

Dynamic light scattering

The DLS analysis was made to examine the population size of the K562 exosomes sample. This analysis was performed in an SZ-100-sizer from Horiba Scientific (Irvine, California, USA) using samples with a 50 µg/mL protein concentration and the following parameters, analysis of organic sample particles in water, 25°C, plastic cells, detector at 90º, general load, cut noise of 5 s, ND filter 100% and standard polydispersion. Three measures were performed in each reading. Z-value results represent the average and standard deviation of three independent readings.

AuNPs synthesis and characterization

AuNPs were synthesized and conjugated to oligo ethylene glycol (OEG) and peptides as previously reported.[21–24,26] Briefly, the synthesis of spherical AuNPs (13±2 nm) was performed according to previously described procedures.[27] A hot aqueous solution of trisodium salt (5 mL, 2% (w/v)) was added under stirring to a boiling aqueous solution. Formation of AuNPs was indicated by the formation of a deep red color. After stirring for further 15 mins and cooling to room temperature, AuNPs were filtered using a 0.2 µm syringe filter and stored at 4°C until use. These AuNPs were then caped with (1-mercaptoundec-11-yl) hexathylene

glycol (OEG, MW =526.7 g/mol) by adding 200 µL OEG to 10 mL of AuNPs 5 nM. After stirring for 2 hrs and an over-night incubation at 4°C, excess unbounded OEG was removed by three centrifugations at 14,000×g for 15 mins and AuNPs@OEG re-dispersion in borate buffer (10 mL, 0.01 M, pH9). AuNPs@OEG were then functionalized with antiangiogenic peptide (KATWLPPR), as previously described.[23,27] Succinctly, 100 µL peptide 1 mg/mL in 0.01 M sodium borate, pH9 was added to 5 mL AuNPs@OEG 1.5 nM in 0.01 M sodium borate buffer, pH9. After addition of 50 µL 1-(3-(dimethylamino)propyl)-3-ethyl-carbodiimide methiodide 0.2 M in water, and 100 µL sulfo-*N*-hydroxysulfosuccinimide 0.2 M in water, the mixture was shaken for 24 hrs at RT, purified by three centrifugations at 16,400 rpm for 15 mins, re-dispersed in water and lyophilized. Confirmation of the functionalization of the antiangiogenic-AuNPs (AuNPs coated with OEG and functionalized with antiangiogenic peptide) was performed using UV-Vis and DLS as described elsewhere.[21,22]

Ex-ovo CAM assays

The CAM assays were performed in agreement with the Directive 2010/63/EU of the European Parliament and of the council of 22 September 2010 on the protection of animals used for scientific purposes and, by using this alternative animal model, obeying to the "3Rs policy" for animal experiments. Fertilized eggs were acquired from Pinto Valouro (Bombarral, Portugal).

The CAM experiments proceeded according to a previously described protocol with minor modifications.[21,28] After 72 hrs incubation at 37°C, 90% (v/v) relative humidity, fertilized eggs were gently opened into white weighing boats (L89xP89xA25mm) covered with an identical punctured weighing boat, allowing the yolk sack blood vessels to be faced upwards. Eggs were allowed to stabilize for another 24 hrs at 37°C, 90% (v/v) relative humidity, and four silicone O-rings (inside diameter 8 mm) were placed equidistantly above the blood vessels of the same embryo, unless otherwise stated. If the embryo showed evidence of severe stress (eg, under-development), they were not considered for analysis. As control, 40 µL of PBS was added to the respective O-ring. Images of the O-ring interior were acquired at specific time-points as indicated using a digital USB Microscope Camera (Opti-Tekscope OT-V1). Firstly, the internal area of the O-ring was selected and image analysis performed using FIJI software as described before.[21] The percentage of newly formed vessels, which were considered exclusively as vessels with lower caliber sprouting from primary or secondary vessels, was calculated relatively to the 0 hrs time point and to the number of newly formed arterioles in the negative control.

Specific details of each set of experiments as indicated:

Effect of K562 derived exosomes on angiogenesis

To assess the effect of CML-derived exosomes in angiogenesis, CAMs were challenged with different amounts of K562 exosomes corresponding to 5 µg/mL or 50 µg/mL total protein inside different O-rings of the same chicken embryo. Eggs (total 11) were then incubated at 37°C, 90% (v/v) relative humidity. Images of the O-ring interior were acquired at 0, 24, 48, and 72 hrs.

Effect of antiangiogenic-AuNPs

To each O-ring placed on the yolk sac membrane of the same chicken embryo, it was inserted 40 µL of 1) PBS; 2) 50 µg/mL of Fibroblasts derived exosomes suspension, 3) 50 µg/mL of K562 derived exosomes suspension, or 4) a mixture of 50 µg/mL of K562 derived exosomes suspension with 16.4 nM antiangiogenic-AuNPs (0.01 pmol/µL for final peptide concentration).[21] Embryos (total 8) were incubated at 37°C, 99% (v/v) relative humidity and images of the O-ring interior acquired at 0, 24, and 48 hrs.

mRNA expression analysis

Gene expression analysis was performed as previously described.[22] To ensure that no cross-effect between challenges was observed, every O-ring of each embryo was infused with the same stimulus. After 12 and 24 hrs incubation at 37°C, 99% (v/v) relative humidity, CAMs were excised and transferred to a microfuge tube. Total RNA was extracted using NZYol reagent (NZYtech, Lisbon, PT), according to the manufacturer's instructions. cDNA synthesis and amplification of Glyceraldehyde 3-phosphate dehydrogenase (*GAPDH* coding for GAPDH), interleukin-8 (*IL8* coding for IL-8), vascular endothelial growth factor A (*VEGFA* coding for VEGFA) , and vascular endothelial growth factor receptor 1 (*FLT1/VEGFR1* coding for VEGFR-1) were performed as previously described, using NZY qPCR green master mix (NZYtech).[22] *IL8, VEGFA*, and *VEGFR1* expression were analyzed using the Ct method ($2^{-\Delta\Delta Ct}$), with *GAPDH* as housekeeping gene and samples treated with PBS as control.[29] It was considered as significantly altered expression when $2^{-\Delta\Delta Ct}$ was higher than 2 or lower than 0.5.

Statistical analysis

Presented results are the mean ± standard error of at least three independent experiments. Statistically, difference was considered for p-value <0.05 calculated using Student t-test, or other unpaired t-test specified in the results section. Statistical analysis was performed using GraphPad prism vs 7.00 (GraphPad Software, Inc, San Diego, CA, USA).

Results

Exosomes isolation and characterization

CML-derived exosomes were isolated from K562 cells in exponential growth. Confirmation of exosome presence in vesicle containing supernatant was achieved via Western-blot for identification of CD-81 protein, a distinctive marker of exosomes (Figure S1A and B). DLS analysis showed that the particle dispersion of the solution revealed a gaussian curve with a peak below 100 nm (Figure S1C), with a Z-value of 70.3±2.6 nm, confirming isolation of exosomes. Together, these data indicate successful isolation of exosomes from K562 cultured cells and the total protein concentration of exosomes solutions was determined (further used as a surrogate indicator of exosome concentration).[12,14]

Effect of K562 exosomes on angiogenesis

An ex-ovo CAM assay was used to assess the effect of K562 exosomes on angiogenesis. O-rings were placed on different locations of the CAM (Figure 2A) and filled with K562 exosomes (0, 5, or 50 µg/mL). Following incubation, the percentage of newly formed arterioles was calculated by normalizing the number of tertiary vessels in the K562 exosomes treated areas (Figure 2C and D) to the number of tertiary vessels of the areas treated with control, ie, PBS (Figure 2B).

Results showed that exposing the yolk sack membrane to low amounts of exosomes (5 µg/mL) did not induce a significant increase of newly formed vessels after 24 hrs incubation (Figure 2B, C, and E). However, an increased exposure to exosome concentration (50 µg/mL) doubled the number of newly formed arterioles for the same period of time (Figure 2B, D, and E). At 72 hrs, the effect of exosomes in forming new vessels decreased to the basal level (Figure 2E). These results agree with those obtained by Mineo et al, where it was observed that treatment of HUVEC with 5 µg/mL K562 derived exosomes resulted only in morphological alteration of the cells, while treatment with a higher concentration (10 µg/mL) caused the development of a tube network.[14]

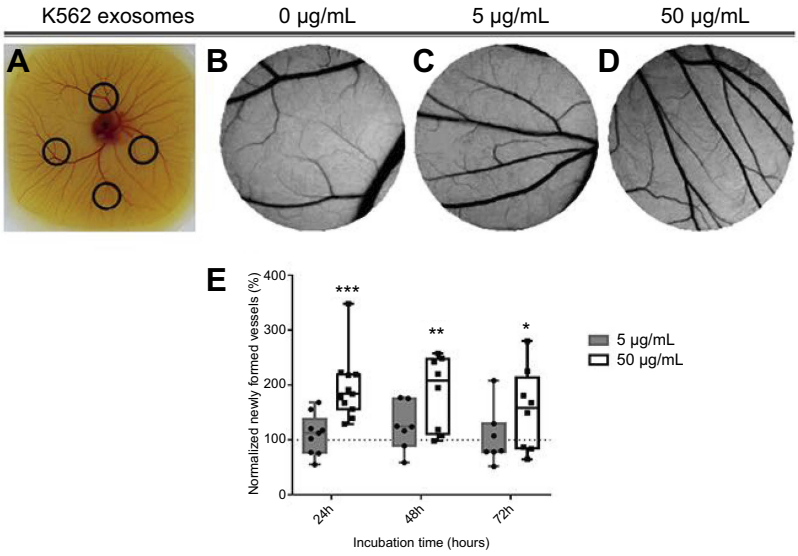

Figure 2 Image of the chicken embryo aspect (**A**) and of the interior of each O-ring placed on the chorioallantoic membrane (CAM). Images were acquired after 24 hrs incubation with 0 µg/mL (**B**), 5 µg/mL (**C**) or, 50 µg/mL (**D**) of K562 derived exosomes. Whiskers plots of the percentage of newly formed vessels after exposure to 5 µg/mL (gray bars) or 50 µg/mL (black and white bars) of K562 exosomes (**E**). Bars represent the maximum, minimal, and mean of at least seven independent experiments, represented as dots (5 µg/mL) and squares (50 µg/mL), normalized to the number of tertiary veins obtained after exposure to phosphate buffer saline (PBS) and to the normalized number obtained in the corresponding CAM area at 0 hrs incubation in the same embryo. Dotted line at 100% normalized newly formed vessels refers to the control sample – number of tertiary veins obtained after exposure to PBS and to the normalized number obtained in the corresponding CAM area at 0 hrs incubation. ***p-value 0.0003, **p-value 0.0056, *p-value 0.13 comparing to the CAM regions exposed to PBS. p-value was calculated using an unpaired t-test with Welch's correction.
Abbreviation: PBS, phosphate buffer saline.

Effect of antiangiogenic-AuNPs

Antiangiogenic-AuNPs with a core diameter of 13±2 nm were synthesized, coated with OEG for increased stability and biocompatibility and conjugated with the antiangiogenic peptide KATWLPPR.[21,22,30] Efficient functionalization was confirmed by UV-Vis spectroscopy and DLS (Figure S2A and B).

To understand if the antiangiogenic-AuNPs were able to counteract the effect on vessel formation induced by K562 derived exosomes, the O-rings were placed on the yolk sack of chicken embryos, and challenged with four different suspensions: PBS (control); Exosomes from K562 cells (50 µg/mL); Exosomes from fibroblasts (50 µg/mL); and a mixture of K562 exosomes (50 µg/mL) and 16.4 nM antiangiogenic-AuNPs. Since human fibroblasts are a healthy type of cells, exosomes derived thereof were used as a negative control. After incubation for 24 and 48 hrs, images of the interior of each O-ring were acquired (Figure 3A) and the percentage of newly formed vessels was calculated regarding the number of branches in each image (Figure 3B).

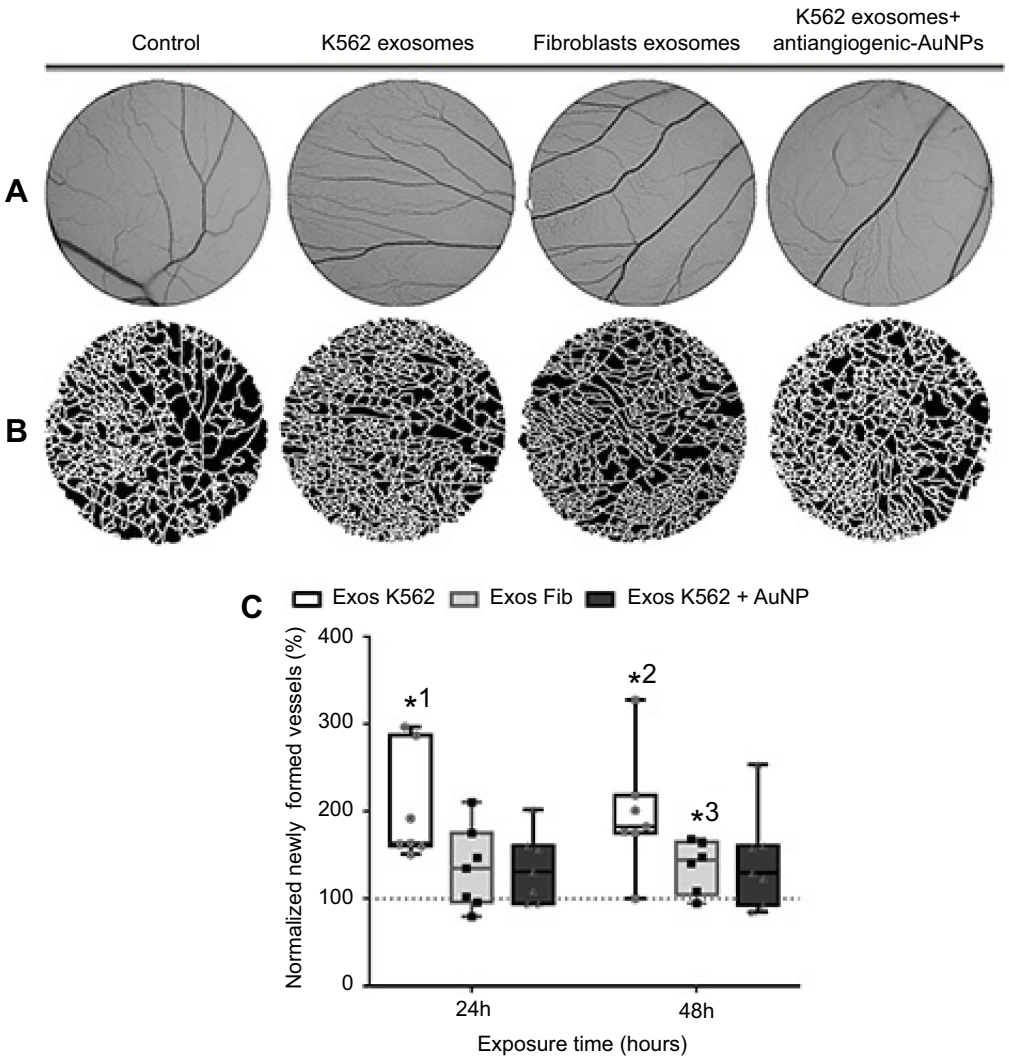

Figure 3 Aspect of the CAM areas treated for 24 hrs with phosphate buffer saline (PBS, control), Exosomes from K562 cells (50 µg/mL), Exosomes from fibroblasts (50 µg/mL), and a mixture of K562 exosomes (50 µg/mL) and 16.4 nM antiangiogenic-AuNPs. (**A**) Green channel images of the CAM region. (**B**) Respective segmented image used to calculate the number of branches. (**C**) Whiskers plots of the percentage of newly formed vessels obtained 24 and 48 hrs after exposure to Exosomes from K562 cells (50 µg/mL) (Exos K562, black bars with white filling); Exosomes from fibroblasts (50 µg/mL) (Exos Fib, gray bars with light gray filling); a mixture of K562 exosomes (50 µg/mL) and 16.4 nM antiangiogenic-AuNPs (Exos K562+ AuNP, black bars with dark gray filling). Bars represent the maximum, minimal, and mean of at least six independent experiments, represented as dots (Exos K562), squares (Exos Fib), or triangles (Exos K562+ AuNP) normalized to the number of tertiary venules obtained in the corresponding CAM area at 0 hrs incubation in the same embryo and to the number of venules obtained after exposure to PBS. Dotted line at 100% normalized newly formed vessels refers to the control sample – number of tertiary venules obtained after exposure to PBS and to the normalized number obtained in the corresponding CAM area at 0 hrs incubation. $*^1$ *p*-value 0.0113, $*^2$ *p*-value 0.0212, $*^3$ *p*-value 0.040 relative to control.

Abbreviations: CAM, chorioallantoic membrane; PBS, phosphate buffer saline.

At 24 hrs, exosomes derived from fibroblasts had no effect in angiogenesis as expected (Figure 3C). However, as shown above, the exosomes derived from K562 cells were able to induce clear increase to the number of newly formed vessels. Once these exosomes are administered together with the anti-angiogenic-AuNPs, the angiogenic effect of exosomes could be completely blocked (Figure 3C), with a percentage of newly formed vessels similar to that of the negative control.

Previous studies report a direct correlation between VEGFR and VEGF mRNA levels and respective protein levels, leading to the resultant vein phenotypic features.[26,31,32] We have previously demonstrated that antiangiogenic-AuNPs were capable to block the connection between VEGFR-1 and NRP-1, resulting in decreased expression of several genes, such as VEGF-A, HIF-1alpha, or c-MYC.[22,26] The characterization of phenotypic alteration, ie, decrease/increase of number of emerging veins directly correlates to the modulation of the respective pathway. To get insights into the mechanism of antiangiogenic-AuNPs blockage of K562 derived exosomes, the expression of some pivotal genes in the angiogenesis process (eg, *IL8, VEGFR1*, and *VEGFA*) was analyzed. Three sets of chicken embryos were prepared with the O-rings were placed equidistantly on the CAM to ensure that each embryo is infused by only one treatment: PBS; K562 exosomes (50 µg/mL) (Exos K562); and a mixture of K562 exosomes (50 µg/mL) and 16.4 nM antiangiogenic-AuNPs (Exos K562+ AuNP). After 12 and 24 hrs incubation, the CAM was excised, and total RNA extracted to assess mRNA levels (gene expression) using the $2^{-\Delta\Delta Ct}$ method by normalization with CAMs treated with PBS (Figure 4).

A 12-hr exposure to K562 exosomes resulted in almost 200-fold increase of *VEGFR1*, while expression of *IL8* and *VEGFA* remained similar to that of the control (Figure 4). These data clearly indicate the triggering of the *VEGFR1* dependent pathway to induce neo-angiogenesis. After 24 hrs incubation, the mRNA levels were similar to the PBS treated sample (control) (Figure 4B). These data are in total agreement with those of the percentage of newly formed vessels over time (Figure 2), suggesting that K562 exosomes induce angiogenesis within the first hours of incubation. What is more, data show that the antiangiogenic-AuNPs block the action of the angiogenic exosomes by silencing of the *VEGFR1* mediated pathways.

Discussion

The pro-angiogenic effect of K562 derived exosomes was demonstrated in the highly complex vasculature system of the CAM. Data show that exosomes trigger a time-dependent effect upon the induction of vessel formation. These findings corroborate in vivo with those previously attained for K562 exosome pro-angiogenic effects using in vitro models.[11] In fact, K562 exosomes are capable to induce a two-fold increase to new vessel formation.

The gene expression profiles highlight the involvement of VEGF-related pathway. The increased expression of VEGF receptor is in line with observations made by Mineo and co-workers who reported that neovascularization in HUVEC mediated by K562 exosomes is dependent on Src, a family of protein tyrosine kinases involved in cellular signaling.[14] Despite this protein being located next to VEGFR-2 (*FLK-1*)

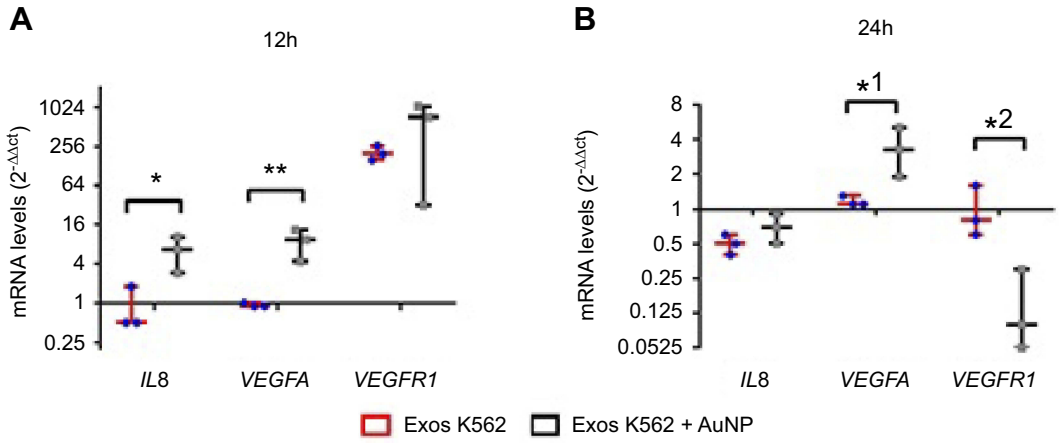

Figure 4 Whiskers plots of *IL8, VEGFA* , and *VEGFR1* mRNA levels after (**A**) 12 hrs and (**B**) 24 hrs of CAM exposure to Exosomes from K562 cells (50 µg/mL) (Exos K562, red bars with blue dots), or a mixture of K562 exosomes (50 µg/mL) and 16.4 nM antiangiogenic-AuNPs (Exos K562+ AuNP, black bars with gray squares). Data were normalized relatively to *GAPDH* mRNA levels and subsequent normalization with CAM treated with PBS. With this procedure, PBS (control) equals to 1 for all analyzed proteins. **p*-value 0.014, ***p*-value 0.004, *[1] *p*-value 0.035, *[2] *p*-value 0.022 relative to the same gene in CAM treated with exosomes alone.
Abbreviations: CAM, chorioallantoic membrane; PBS, phosphate buffer saline.

in the VEGF signaling pathway, studies on human retinal microvascular endothelial cells suggested that VEGFR-1 activation also mediates neovascularization through the Src-PLD1-PKCγ-cPLA2 signaling pathway.[33,34] The time and dose-dependence on HUVEC differentiation mediated by LAMA84 derived exosomes were also observed by Taverna et al[11]. However, contrary to the results obtained by Taverna et al, who observed an increased expression of *IL8* in HUVEC after exposure to K562 exosomes, the expression of *IL8* in the highly vascularized CAM remained identical to the control (Figure 4).[11] It should be noted that these studies were performed with distinct approaches: an in vitro study, where HUVECs are completely exposed to K562 exosomes; whereas in the herein presented CAM assay, exosomes must pass through the epithelium to reach the stroma where the blood vasculature reside together with lymphatic system.[28] Moreover, the endothelial cells environments are relevant to the proinflammatory response.[35]

When CAMs were simultaneously exposed to K562 exosomes and antiangiogenic-AuNPs, the percentage of newly formed vessels was the same as for the untreated control, suggesting that the K562 exosomes pro-angiogenic effect was blocked by the peptides grafted onto the AuNPs, most likely via a VEGF-dependent cascade. In fact, the antiangiogenic effect of these nanoconjugates has been shown to tackle this relevant pathway in HUVEC and CAM assays.[22–24,26]

The increased expression of *VEGFA*, the agonist of VGFR-1 after 24 hrs exposure to K562 exosomes and antiangiogenic-AuNP is of note. In fact, it would be expected a decrease of *VEGFA* expression with *VEGFR1* as observed by Pedrosa et al[22]. The increased expression of *VEGFR1, IL8* , and *VEGFA* after 12 hrs (Figure 4A) can shed some light on this question, since it suggests a counter-response mediated by the antiangiogenic-AuNP to the presence of K562 exosomes. Exosomes derived from CML cells contain microRNAs involved in angiogenesis modulation, including miR-126 and miR-92a, both miRNAs with high homology between humans and chicken (gga-miR-126 with 100% homology with human miR-126 and gga-miR-92–1 with 93.24% homology with human miR-92a-1).[10,18,36,37] Studies on mice and zebrafish revealed that miR-126 is involved in the regulation of vascular integrity and angiogenesis by repressing negative regulators of the VEGF pathway, including sprout-related protein, SPRED1, and phosphoinositol-3 kinase regulatory subunit, PIK3R2/p85-beta.[38,39] Treatment of HUVEC with K562 exosome-mediated miR92a suggested that this miRNA is involved in endothelial cells migration and tube formation.[18]

Our results suggest that CAM exposure to K562 exosomes activates the VEGF pathway, resulting in an increased expression of *VEGFR1* (Figure 4A). The inhibition of NRP-1 mediated by the nanoconjugate[21,22] exacerbates the CAM response to the angiogenic activation by K562 exosomes, triggering an increase of angiogenic mediators, including *IL8, VEGFA*, and *VEGFR1* (Figure 4A). As the K562 exosomes effect fades out with time, the effect of the antiangiogenic-AuNPs became preponderant, thus decreasing the expression of *VEGFR1*. One might consider that, when the number of newly formed vessels were accounted (Figure 3C), the effect of the antiangiogenic-AuNP had already balanced initial trigger by the K562, and thus the percentage of newly formed vessels was similar to that of the control. Regardless of the underlying mechanisms inherent to gene expression alterations, the phenotypic features prevail and the effect of the nanoconjugates was proven effective to inhibit the neo-angiogenesis mediated by CML-derived exosomes.

Conclusion

Herein, we demonstrate the capability of CML-derived exosomes to trigger neo-angiogenesis in vivo, which has got severe implications for understanding tumor development, providing cues for biomarkers of prognosis and eventual antiangiogenic therapeutic strategies. What is more, by using antiangiogenic-AuNP we were capable to counteract the effect of CML-derived exosomes in creating new vessels. This approach may provide for an easy to use tool to assist further studies for the molecular pathways of exosome transforming effects in cancer, which in turn might have relevant implication toward the development of innovative therapy strategies capable to tackle the bone marrow tumor microenvironment in CML patients.

Abbreviations

AuNPs, gold nanoparticles; AuNPs@OEG, gold nanoparticles functionalized with OEG; CAM, chorioallantoic membrane; CML, chronic myeloid leukemia; DLS, dynamic light scattering; DMEM, dulbecco´s modified eagle medium; EGF, epidermal growth factor; FBS, fetal bovine serum; GAPDH, glyceraldehyde 3-phosphate dehydrogenase; HUVEC, human umbilical vein endothelial cells; IL-8, interleukin 8; NRP-1, neuropilin-1 receptor; OEG, oligo ethylene glycol ((1-mercaptoundec-11-yl) hexathylene glycol)); PBS, phosphate buffer saline; TKIs, tyrosine kinase inhibitors; VEGF, vascular endothelial growth factor; VEGFR, VEGF receptor.

Acknowledgments

This work was supported by the Applied Molecular Biosciences Unit – UCIBIO which is financed by national funds from FCT/MCTES (UID/Multi/04378/2019). CRR also acknowledges FCT/MCTES through SFRH/BPD/124612/2016.

Disclosure

The authors report no conflicts of interest in this work.

References

1. Jabbour E, Kantarjian H. Chronic myeloid leukemia: 2018 update on diagnosis, therapy and monitoring. *Am J Hematol*. 2018;93(3):442–459. doi:10.1002/ajh.25011
2. Kang ZJ, Liu YF, Xu LZ, et al. The Philadelphia chromosome in leukemogenesis. *Chin J Cancer*. 2016;35:48. doi:10.1186/s40880-016-0108-0
3. Korkolopoulou P, Viniou N, Kavantzas N, et al. Clinicopathologic correlations of bone marrow angiogenesis in chronic myeloid leukemia: a morphometric study. *Leukemia*. 2003;17(1):89–97. doi:10.1038/sj.leu.2402769
4. Deshantri AK, Varela Moreira A, Ecker V, et al. Nanomedicines for the treatment of hematological malignancies. *J Control Release*. 2018;287:194–215. doi:10.1016/j.jconrel.2018.08.034
5. Rackov G, Garcia-Romero N, Esteban-Rubio S, Carrion-Navarro J, Belda-Iniesta C, Ayuso-Sacido A. Vesicle-mediated control of cell function: the role of extracellular matrix and microenvironment. *Front Physiol*. 2018;9:651. doi:10.3389/fphys.2018.00651
6. Roma-Rodrigues C, Fernandes AR, Baptista PV. Exosome in tumour microenvironment: overview of the crosstalk between normal and cancer cells. *Biomed Res Int*. 2014;2014:179486. doi:10.1155/2014/179486
7. Sauter ER. Exosomes in blood and cancer. *Transl Cancer Res*. 2017;6(S8):S1316–S1320. doi:10.21037/tcr.2017.08.13
8. Sauter ER. Exosomes in lymph and cancer. *Transl Cancer Res*. 2017;6(S8):S1311–S1315. doi:10.21037/tcr.2017.10.06
9. Qiu JJ, Lin XJ, Tang XY, Zheng TT, Lin YY, Hua KQ. Exosomal metastasis-associated lung adenocarcinoma transcript 1 promotes angiogenesis and predicts poor prognosis in epithelial ovarian cancer. *Int J Biol Sci*. 2018;14(14):1960–1973. doi:10.7150/ijbs.28048
10. Aslan C, Maralbashi S, Salari F, et al. Tumor-derived exosomes: implication in angiogenesis and antiangiogenesis cancer therapy. *J Cell Physiol*. 2019;234:16885–16903. ahead of print. doi:10.1002/jcp.28374
11. Taverna S, Flugy A, Saieva L, et al. Role of exosomes released by chronic myelogenous leukemia cells in angiogenesis. *Int J Cancer*. 2012;130(9):2033–2043. doi:10.1007/s10456-011-9241-1
12. Roma-Rodrigues C, Pereira F, Alves de Matos AP, Fernandes M, Baptista PV, Fernandes AR. Smuggling gold nanoparticles across cell types – a new role for exosomes in gene silencing. *Nanomedicine*. 2017;13(4):1389–1398. doi:10.1016/j.nano.2017.01.013
13. Taverna S, Amodeo V, Saieva L, et al. Exosomal shuttling of miR-126 in endothelial cells modulates adhesive and migratory abilities of chronic myelogenous leukemia cells. *Mol Cancer*. 2014;13:169. doi:10.1186/1476-4598-13-169
14. Mineo M, Garfield SH, Taverna S, et al. Exosomes released by K562 chronic myeloid leukemia cells promote angiogenesis in a Src-dependent fashion. *Angiogenesis*. 2012;15(1):33–45. doi:10.1007/s10456-011-9241-1
15. Tadokoro H, Umezu T, Ohyashiki K, Hirano T, Ohyashiki JH. Exosomes derived from hypoxic leukemia cells enhance tube formation in endothelial cells. *J Biol Chem*. 2013;288(48):34343–34351. doi:10.1074/jbc.M113.480822
16. Corrado C, Saieva L, Raimondo S, Santoro A, De Leo G, Alessandro R. Chronic myelogenous leukemia exosomes modulate bone marrow microenvironment through activation of epidermal growth factor receptor. *J Cell Mol Med*. 2016;20(10):1829–1839. doi:10.1111/jcmm.12873
17. Raimondo S, Saieva L, Corrado C, et al. Chronic myeloid leukemia-derived exosomes promote tumor growth through an autocrine mechanism. *Cell Commun Signal*. 2015;13:8. doi:10.1186/s12964-015-0086-x
18. Umezu T, Ohyashiki K, Kuroda M, Ohyashiki JH. Leukemia cell to endothelial cell communication via exosomal miRNAs. *Oncogene*. 2013;32(22):2747–2755. doi:10.1038/onc.2012.295
19. Vinhas R, Mendes R, Fernandes AR, Baptista PV. Nanoparticles-emerging potential for managing leukemia and lymphoma. *Front Bioeng Biotechnol*. 2017;5:79. doi:10.3389/fbioe.2017.00079
20. Soni G, Yadav KS. Applications of nanoparticles in treatment and diagnosis of leukemia. *Mater Sci Eng C Mater Biol Appl*. 2015;47:156–164. doi:10.1016/j.msec.2014.10.043
21. Roma-Rodrigues C, Heuer-Jungemann A, Fernandes AR, Kanaras AG, Baptista PV. Peptide-coated gold nanoparticles for modulation of angiogenesis *in vivo*. *Int J Nanomedicine*. 2016;11:2633–2639. doi:10.2147/IJN.S108661
22. Pedrosa P, Heuer-Jungemann A, Kanaras AG, Fernandes AR, Baptista PV. Potentiating angiogenesis arrest in vivo via laser irradiation of peptide functionalized gold nanoparticles. *J Nanobiotechnology*. 2017;15(1):85. doi:10.1186/s12951-017-0321-2
23. Bartczak D, Sanchez-Elsner T, Louafi F, Millar TM, Kanaras AG. Receptor-mediated interactions between colloidal gold nanoparticles and human umbilical vein endothelial cells. *Small*. 2011;7(3):388–394. doi:10.1002/smll.201001816
24. Bartczak D, Muskens OL, Sanchez-Elsner T, Kanaras AG, Millar TM. Manipulation of in vitro angiogenesis using peptide-coated gold nanoparticles. *ACS Nano*. 2013;7(6):5628–5636. doi:10.1021/nn402111z
25. Herzog B, Pellet-Manya C, Brittona G, Hartzoulakis B, Zachary IC. VEGF binding to NRP1 is essential for VEGF stimulation of endothelial cell migration, complex formation between NRP1 and VEGFR2, and signaling via FAK Tyr407 phosphorylation. *Mol Biol Cell*. 2011;22(15):2766–2776. doi:10.1091/mbc.E09-12-1061
26. Bartczak D, Sanchez-Elsner T, Louafi F, Millar TM, Kanaras AG. Receptor-mediated interactions between colloidal gold nanoparticles and human umbilical vein endothelial cells. *Small*. 2010;7(3):388–394. doi:10.1002/smll.201001816
27. Bartczak D, Muskens OL, Nitti S, Millar TM, Kanaras AG. Nanoparticles for inhibition of *in vitro* tumour angiogenesis: synergistic actions of ligand function and laser irradiation. *Biomater Sci*. 2015;3(5):733–741. doi:10.1039/C5BM00053J
28. Nowak-Sliwinska P, Segura T, Iruela-Arispe ML. The chicken chorioallantoic membrane model in biology, medicine and bioengineering. *Angiogenesis*. 2014;17(4):779–804. doi:10.1007/s10456-014-9440-7
29. Livak KJ, Schmittgen TD. Analysis of relative gene expression data using real-time quantitative PCR and the 2(-Delta Delta C(T)) Method. *Methods*. 2001;25(4):402–408. doi:10.1006/meth.2001.1262
30. Turkevich J, Stevenson PC, Hillier J. A study of the nucleation and growth processes in the synthesis of colloidal gold. *Discuss Faraday Soc*. 1951;11:55–75. doi:10.1039/DF9511100055
31. Zhang Z, Neiva KG, Lingen MW, Ellis MW, Nör JE. VEGF-dependent tumor angiogenesis requires inverse and reciprocal regulation of VEGFR1 and VEGFR2. *Cell Death Differ*. 2010;17(3):499–512. doi:10.1038/cdd.2009.152
32. Sekiguchi K, Ito Y, Hattori K, et al. VEGF receptor 1-expressing macrophages recruited from bone marrow enhances angiogenesis in endometrial tissues. *Sci Rep*. 2019;9(1):7037. doi:10.1038/s41598-019-43185-8
33. Chou MT, Wang J, Fujita DJ. Src Kinase becomes preferentially associated with the VEGFR, KDR/Flk-1, following VEGF stimulation of vascular endothelial cells. *BMC Biochem*. 2002;3:32. doi:10.1186/1471-2091-3-32

34. Singh NK, Hansen DE 3rd, Kundumani-Sridharan V, Rao GN. Both Kdr and Flt1 play a vital role in hypoxia-induced Src-PLD1-PKCgamma-cPLA(2) activation and retinal neovascularization. *Blood*. 2013;121(10):1911–1923. doi:10.1182/blood-2012-03-419234
35. Nash GB, Buckley CD, Ed Rainger G. The local physicochemical environment conditions the proinflammatory response of endothelial cells and thus modulates leukocyte recruitment. *FEBS Lett*. 2004;569 (1–3):13–17. doi:10.1016/j.febslet.2004.05.040
36. Ohyashiki JH, Umezu T, Ohyashiki K. Exosomes promote bone marrow angiogenesis in hematologic neoplasia: the role of hypoxia. *Curr Opin Hematol*. 2016;23(3):268–273. doi:10.1097/MOH.0000000000000235
37. Anand S, Cheresh DA. MicroRNA-mediated regulation of the angiogenic switch. *Curr Opin Hematol*. 2011;18(3):171–176. doi:10.1097/MOH.0b013e328345a180
38. Fish JE, Santoro MM, Morton SU, et al. miR-126 regulates angiogenic signaling and vascular integrity. *Dev Cell*. 2008;15(2):272–284. doi:10.1016/j.devcel.2008.07.008
39. Wang S, Aurora AB, Johnson BA, et al. The endothelial-specific microRNA miR-126 governs vascular integrity and angiogenesis. *Dev Cell*. 2008;15(2):261–271. doi:10.1016/j.devcel.2008.07.002

Supplementary materials

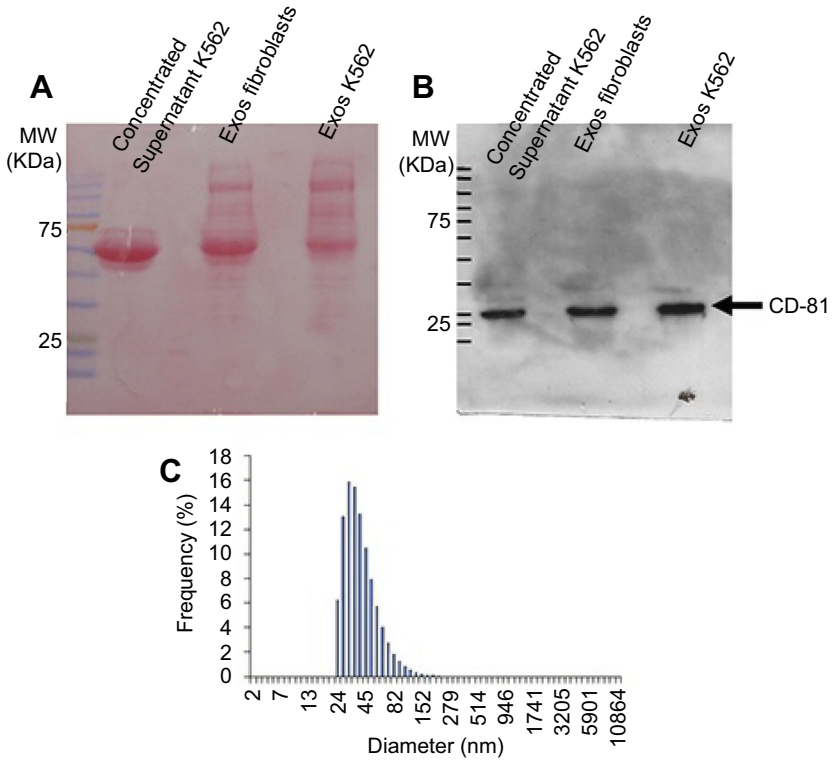

Figure S1 Evaluation of exosome isolation. Supernatant of Fibroblasts and K562 cells was collected, filtered in a 0.2μm filter and concentrated in Centrifugal Filter Devices with 3KW cut-off. An aliquot of the K562 concentrated supernatant was collected and analysed (Concentrated supernatant K562). Total exosome isolation reagent for culture media (ThermoFisher) was added to each concentrated supernatant and exosomes collected according to the manufacturer's instructions (Exos Fibroblasts and Exos K562). For Western-Blot analysis, 40μg of protein from each sample was separated by SDSPAGE, transferred to a PVDF membrane and stained with Ponceau solution (**A**). The presence of CD-81 tetraspanin was then analysed with CD-81 antibody (1D6, Novus biologicals Cat# NB100-65805, RRID:AB_962702) (**B**). The expected weight of CD-81 is 26KDa. Dynamic light scattering of particle distribution in K562 exosome suspension (**C**).

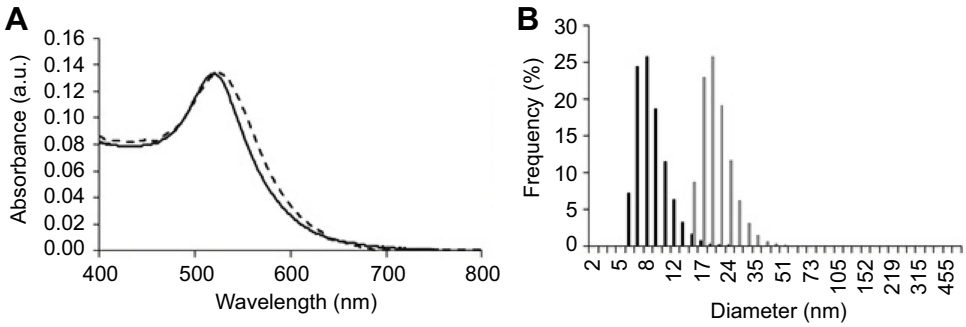

Figure S2 Characterisation of the antiangiogenic-AuNPs. (**A**) UV–Vis spectra of AuNPs (continuous black line) and antiangiogenic-AuNPs (doted grey line). A red shift of the surface plasmon resonance peak in the UV–Vis spectrum infers successful functionalisation with the peptide. (**B**) Dynamic light scattering with diameter distribution of AuNPs (black bars), with an average diameter of 17·5±0·4nm, and antiangiogenic-AuNPs (grey bars), with an average diameter of 32·8±0·4nm.